Available online at www.sciencedirect.com
SCIENCE DIRECT®
Materials and Design 27 (2006) 640–650
Materials & Design
www.elsevier.com/locate/matdes

Some aspects on strain hardening behaviour in three dimensions of aluminium–iron powder metallurgy composite during cold upsetting

R. Narayanasamy [a,*], T. Ramesh [b], K.S. Pandey [c]

[a] Department of Production Engineering, National Institute of Technology, Tiruchirappalli 620 015, Tamilnadu, India
[b] Department of Mechanical Engineering, J.J. College of Engineering and Technology, Tiruchirappalli 620 009, Tamilnadu, India
[c] Department of Metallurgical Engineering, National Institute of Technology, Tiruchirappalli 620 015, Tamilnadu, India

Received 21 July 2004; accepted 20 December 2004
Available online 16 February 2005

Abstract

Strain hardening is an important phenomenon, which is required to study the plastic deformation of any material and also it is an important parameter in the study of workability criteria of metals. The present investigation has been undertaken to evaluate the strain hardening phenomenon experienced during the cold working of sintered aluminium–iron powder metallurgy composite performs during upsetting operation under various stress state conditions namely uniaxial, plane and triaxial. Sintered performs of three different aspect ratios namely 0.44, 0.45 and 0.75 with two different per cent of iron contents (0% and 2%) and with three different iron particle sizes namely −53 to +45 μm, −76 to +63 μm and −106 to +90 μm were prepared and cold forged. The strain hardening exponent '*n*' and the strength coefficient '*K*' were obtained for each aspect ratio and iron particle sizes. It is found that there is a greater change in the values of '*n*' and '*K*' for the different addition of iron powders and also for the different iron particle sizes for different aspect ratios and for different stress state conditions.

Keywords: Upsetting; Strain hardening exponent; Strength coefficient; Formability; Triaxial stress; Powder metallurgy

1. Introduction

One of the predominant characteristics of the plastic deformation of metals is the fact that the shear stress required to produce slip continuously increasing shear strain. The increase in the stress required to cause slip because of previous plastic deformation is known as strain hardening, or work hardening [1]. Understanding the behaviour of powder metallurgy compacts is an important area where the researchers have to put much focus of their attention. Ductile fracture is the common mode of failure, which is a complicated phenomenon that is dependent upon process parameters such as stress, strain, strain-rate, friction, etc., and the material parameters such as strain hardening and the volume fraction of voids and second phase particles. Kuhn and Downey [2] investigated the deformation characteristics and the plasticity theory of sintered powder materials and studied the basic deformation behaviour of sintered iron powder performing a simple homogeneous compression tests and also proposed a plasticity theory relating yield stress and Poisson's ratio to the density. A new yield criterion is also proposed for the prediction of forming stresses in repressing and in plane strain compression. A plasticity theory for porous solids was proposed by Green [3] considering numerous cracks or voids in the shape of spherical or where the direction

* Corresponding author. Tel.: +91 0431 2501801; fax: +91 0431 2500133.
E-mail addresses: narayan@nitt.edu (R. Narayanasamy), trhashwek@yahoo.co.in (T. Ramesh), pandey@nitt.edu (K.S. Pandey).

0261-3069/$ - see front matter © 2005 Elsevier Ltd. All rights reserved.
doi:10.1016/j.matdes.2004.12.012

of cracks was completely random. And also an approximate expression for deformation theory was also discussed. Shima and Oyane [4] proposed a plasticity theory for porous metals of sintered copper with various apparent densities and the stress–strain curves for pore free copper compacts were also calculated utilizing the basic equations and compared with the experimental results. Gurson [5] discussed the continuum theory of ductile rupture by void nucleation and growth considering yield criteria and flow rules for porous ductile media and developed approximate yield criteria and flow rules for porous ductile materials by showing the role of hydrostatic stress in plastic yield and void growth. Doraivelu et al. [6] proposed a new yield equation for the P/M materials and verified experimentally the uniaxial state of compressive stress using aluminium alloy and the yield surfaces for various density levels were generated in a three dimensional principal – stress space with the help of computer graphics. Abdel-Rahman and El-Sheikh [7] investigated the effect of relative density on the forming limit of powder metallurgy compacts during upsetting. It is also discussed the effect of density for powder metallurgy deformation characterization adopting Kuhn and Downey theories under uniaxial stress state conditions and suggested that more negative value of β corresponds to a larger strain-to-fracture value and concluded the value of the axial strain (ε) at fracture is a function of the relative density. Two mechanical tests were carried out by Abdel-Rahman [8] for the determination of workability curves. Approximate determination of workability has been carried out using uniaxial tension and uniaxial compression test and a linear relationship between the workability function and the stress formability is proposed.

An excellent research work on the sintered aluminium–iron composite preforms under uniaxial stress state condition was carried out by Narayanasamy and Pandey [9] in order to evaluate the work hardening characteristics. The effect of iron content, iron particle-size range and the initial aspect ratio of the preforms on work hardening were investigated. Inigoraj, Narayanasamy and Pandey [10] studied the strain hardening behaviour of sintered aluminium–alumina composite during axial compression with and without the annealing processes and suggested that the strain hardening exponent 'n' decreases linearly with respect to increased fractional theoretical density and established an empirical relationship between n and fractional theoretical density. The instantaneous strain hardening behaviour due to axial stress of aluminium preforms during cold axial forming under plane stress state condition was investigated by Selvakumar and Narayanasamy [11] and concluded that the initial geometry of the P/M performs plays a predominant role in influencing the strain hardening exponent and the strength coefficient and they achieved the peak values of 'n' and 'K' for the lower value of packing density. Senthilvelan et.al. [12], developed a mathematical model for P/M working process, using regression analysis and analysis of variance in order to study the main interaction effects of process parameters and they verified the mathematical model developed by calculating correlation coefficient and using this model they predicted the strength coefficient (K) and strain hardening exponent (n) and estimated the flow stress of P/M copper performs. Peng and Balendra [13] derived a 3D consecutive equation for large elastoplastic deformation taking into account the energy stored in the residual microstress field in plastically deformed materials and its effect on subsequent plastic deformation and they validated the derived equations through ABAQUS taking necking of a cylindrical bar considering the effect of strain hardening induced by change of specimen geometry during deformation.

In the present work, the instantaneous strain hardening behaviour in different directions of aluminium–iron powder performs under various stress state conditions namely uniaxial, plane and triaxial were completely investigated. The plots for the strain hardening exponent 'n' and the strength coefficient 'K' against the relative density were plotted for various stress state conditions and various content of iron per cent and different particle sizes.

2. Theoretical investigation

The mathematical expressions used and proposed for the determination of various upsetting parameters of upsetting for various stress state conditions are discussed below:

2.1. Uniaxial stress state condition

In the compression of a P/M part, under frictional conditions, the average density is increased. Friction

Table 1
Characteristics of the aluminium powder

Sieve analysis		Characteristics of aluminium powder	
Sieve number	Weight % retained		
+150	2.60	Apparent density (g cm^{-3})	1.030
+125	4.61	Flow rate, S (by Hall flow meter) (50 g)$^{-1}$	32.00
+106	2.00	Compressibility at a 2pressure of 300 Mpa (g cm^{-3})	2.344
+90	1.74		
+75	8.05		
+63	8.20		
+53	15.90		
+45	18.80		
+38	2.64		
−38	33.81		

enhances densification and at the same time decreases the height reduction at fracture. The state of stress in a homogeneous compression process is as follows:

According to Abdel-Rahman et al. [7];

$$\sigma_z = -\sigma_{\text{eff}}, \quad \sigma_r = \sigma_\theta = 0, \tag{1}$$

where σ_z is the axial stress, σ_{eff} is the effective stress, σ_r is the radial stress and σ_θ is the hoop stress.

$$\sigma_m = (\sigma_z/3), \tag{2}$$

where σ_m is the mean or hydrostatic stress. and the strain state is,

$$\varepsilon_\theta = -\varepsilon_{\text{eff}} = \ln(D_f/D_0) \quad \text{and}$$

$$\varepsilon_z = \ln[H_f/H_0], \tag{3}$$

where ε_θ is the hoop strain, ε_z is the axial strian, D_0 is the initial diameter of the compacts, D_f is the contact diameter after deformation, H_0 is the initial height of the compacts and H_f is the fracture height of the compacts.

When the compression continues, the final diameter increases and the corresponding hoop strain, which is tensile in nature, also increases until it reaches the fracture limit. Once the fracture is initiated, the forming lim-

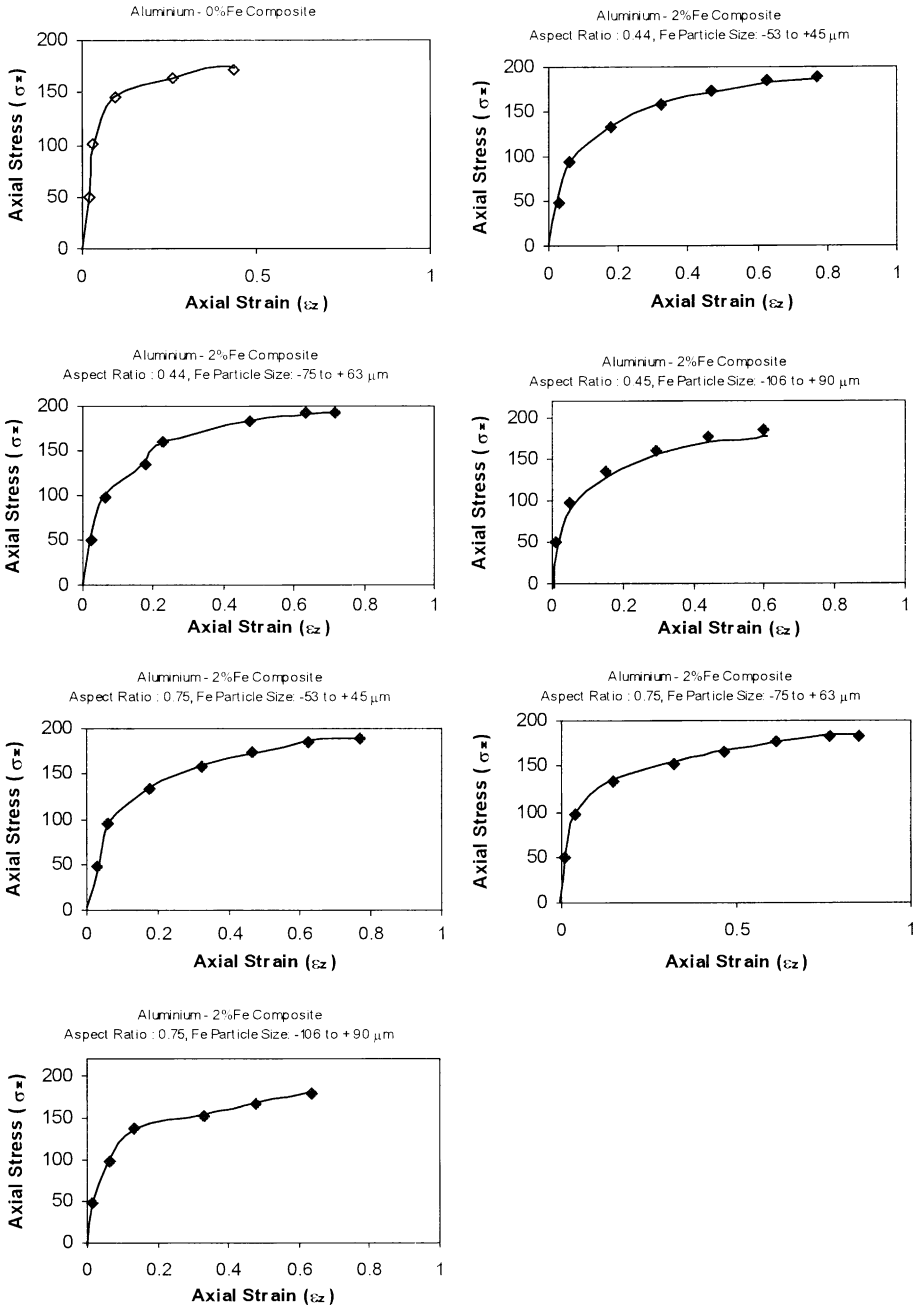

Fig. 1. Axial stress (σ_z) vs. axial strain (ε_z) for various aspect ratios and Fe particle sizes.

it strain is the same as the effective strain. It is determined from;

$$\phi_{\text{eff}} = \ln[H_0/H_f]. \quad (4)$$

As an evidence of experimental investigation implying the importance of the spherical component of the stress state on fracture according to Vujovic and Shabaik [14] proposed a parameter called a Formability Stress Index 'β' is given by,

$$\beta = [3\sigma_m/\sigma_{\text{eff}}], \quad (5)$$

This index determines the fracture limit as explained in the Reference [7].

2.2. Plane stress state condition

According to Narayanasamy and Pandey [15], the state of stress in a plane stress condition is as follows:

$$\sigma_{\text{eff}} = (0.5 + \alpha)[3(1 + \alpha + \alpha^2)]^{0.5}\sigma_z, \quad (6)$$

where σ_{eff} is the effective stress,

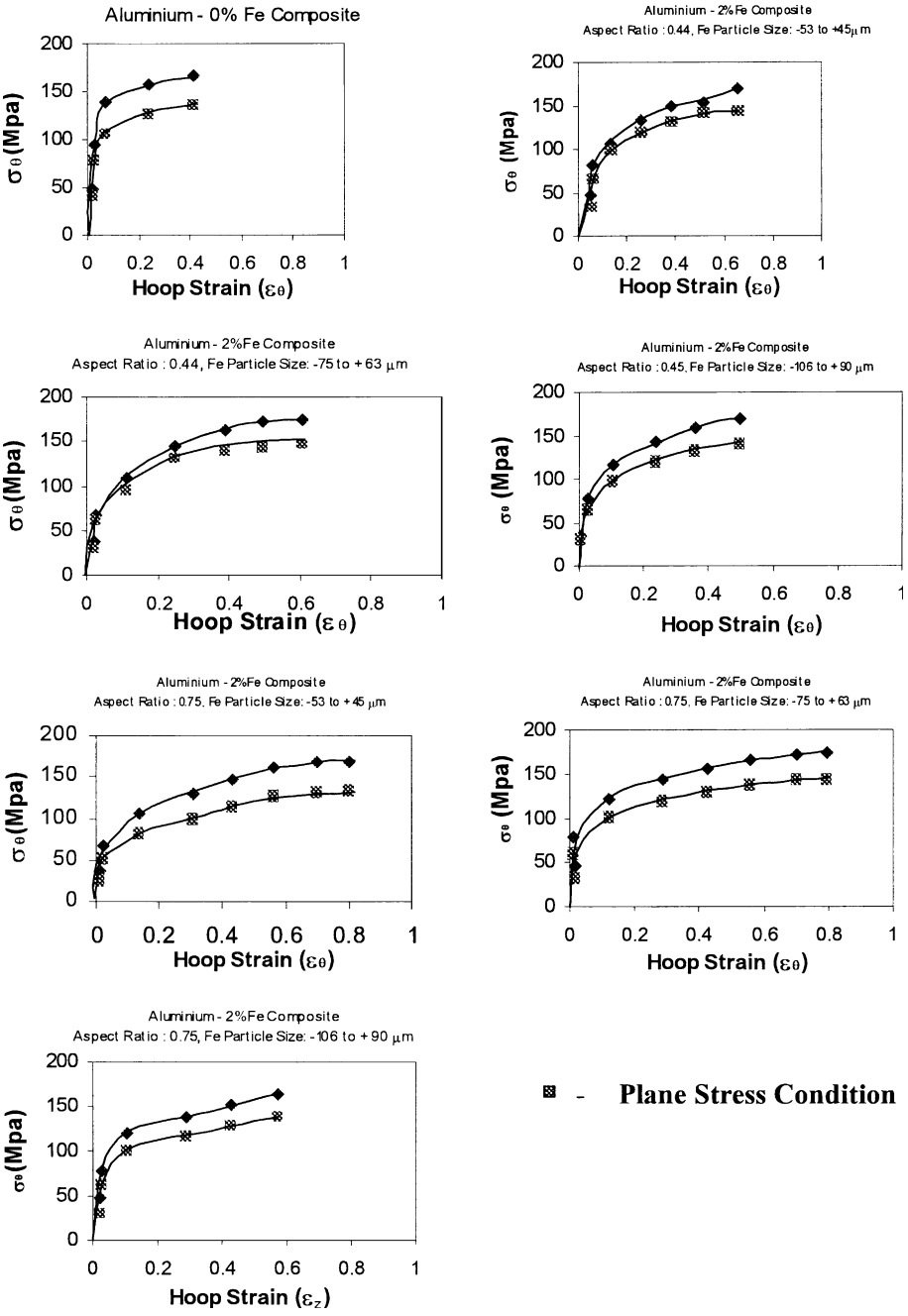

Fig. 2. Hoop stress (σ_θ) vs. hoop strain (ε_θ) for various aspect ratios and Fe particle sizes – comparison between plane and triaxial stress state conditions.

α is the Poisson's ratio $= (\varepsilon_\theta/2\varepsilon_z)$ (7)

and σ_z is the axial stress in upsetting.

Since the radial stress, σ_r is zero at the free surface it follows from the flow rule that,

$$\sigma_\theta = [(1+2\alpha)/(2+\alpha)]\sigma_z \quad (8)$$

and the hydrostatic stress (σ_m) is,

$$\sigma_m = (1/3)[\sigma_\theta + \sigma_z]. \quad (9)$$

The hoop strain (ε_θ) of the compact is determined as explained elsewhere [15].

$$\varepsilon_\theta = \ln[(2D_B^2 + D_c^2)/3D_0^2], \quad (10)$$

where D_B is bulged diameter of the compacts, D_c is contact diameter of the compacts and D_0 is the initial diameter of the compacts.

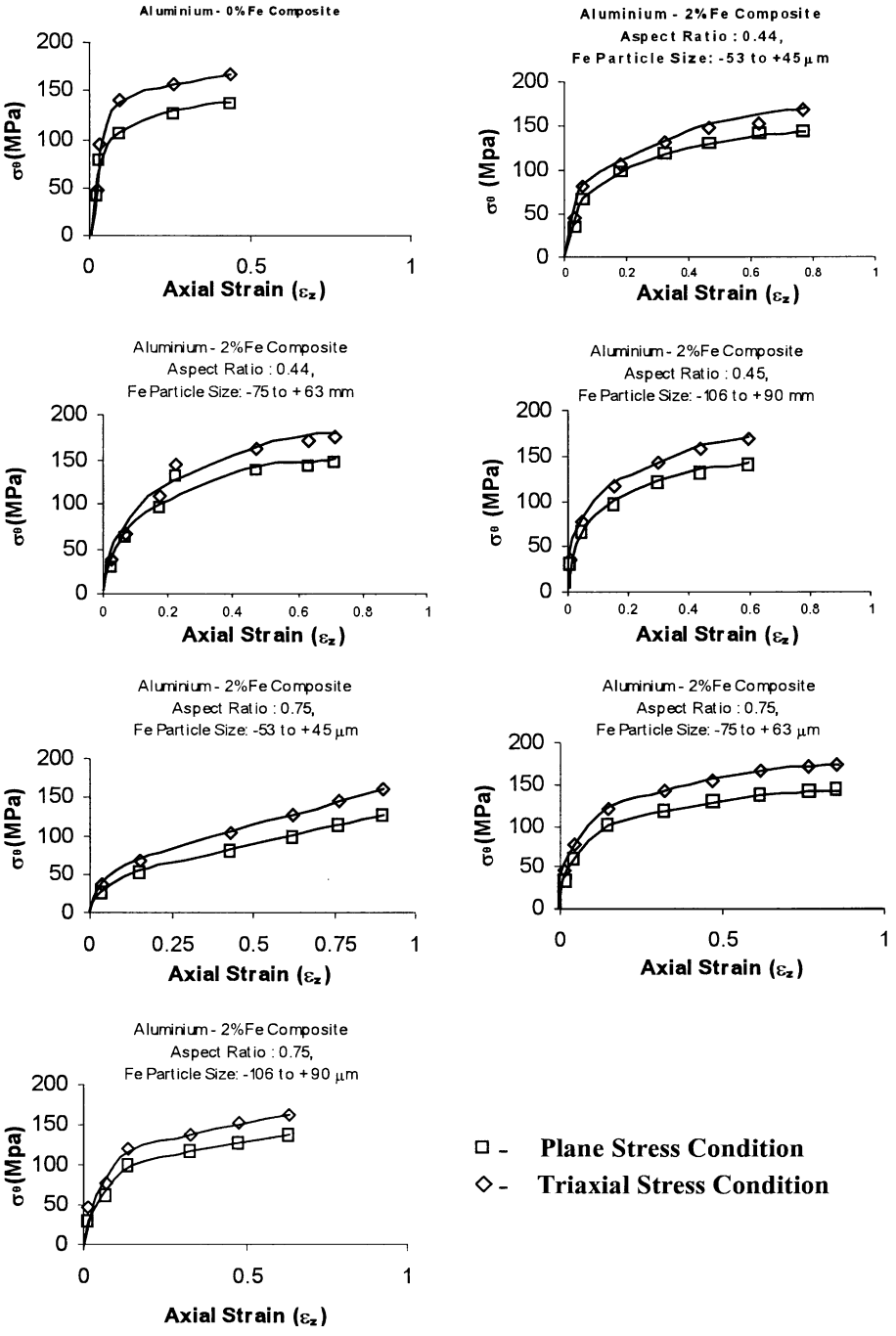

Fig. 3. Hoop stress (σ_θ) vs. axial strain (ε_z) for various aspect ratios and Fe particle sizes – comparison between plane and triaxial stress state conditions.

2.3. Triaxial stress state condition

According to Narayanasamy and Ponalagusamy [16] the state of stress in a triaxial stress condition is given as follows:

$$\alpha = (A/B), \tag{11}$$

where $A = [(2 + R^2)\sigma_\theta - R^2(\sigma_z + 2\sigma_\theta)]$, $B = [(2 + R^2)\sigma_z - R^2(\sigma_z + 2\sigma_\theta)]$, α = Poisson's ratio and R = relative density. From the above Eq. (11), using the known values of α, R and σ_z, the hoop stress component (σ_θ) can be determined as follows:

$$\sigma_\theta = [(2\alpha + R^2)/(2 - R^2 + 2R^2\alpha)]\sigma_z. \tag{12}$$

In the above Eq. (12), the relative density (R) plays a major role in finding the hoop stress component.

Since $\sigma_r = \sigma_\theta$ in case of triaxial stress condition, the hydrostatic stress is given by,

$$\sigma_m = [(\sigma_1 + \sigma_2 + \sigma_3)/3] = [(\sigma_z + 2\sigma_\theta)/3]. \tag{13}$$

The effective stress can be determined from the following relation as explained elsewhere [16]:

$$[\sigma_1^2 + \sigma_2^2 + \sigma_3^2 - R^2(\sigma_1\sigma_2 + \sigma_2\sigma_3 + \sigma_3\sigma_1)] = (2R^2 - 1)\sigma_{\text{eff}}^2 \tag{14}$$

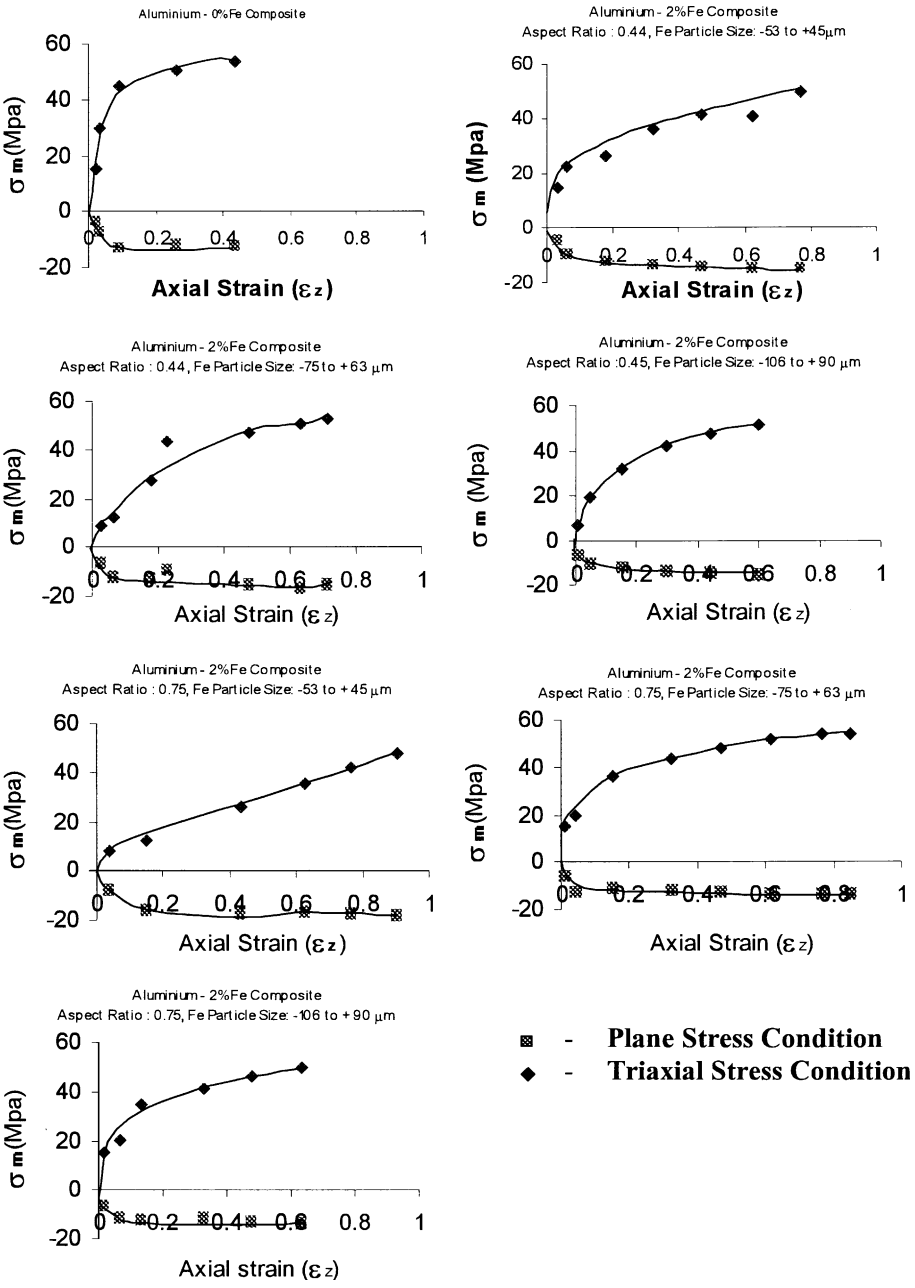

Fig. 4. Hydrostatic stress (σ_m) vs. axial strain (ε_z) for various aspect ratios and Fe particle sizes – comparison between plane stress and triaxial stress state conditions.

(or)

$$\sigma_{\text{eff}}^2 = [(\sigma_z^2 + \sigma_\theta^2 + \sigma_r^2 - R^2(\sigma_z\sigma_\theta + \sigma_\theta\sigma_r + \sigma_r\sigma_z))/(2R^2 - 1)].$$

Since $\sigma_\theta = \sigma_r$:

$$\sigma_{\text{eff}}^2 = [(\sigma_z^2 + 2\sigma_\theta^2 - R^2(\sigma_z\sigma_\theta + \sigma_\theta^2 + \sigma_z\sigma_\theta))/(2R^2 - 1)],$$

$$\sigma_{\text{eff}} = [(\sigma_z^2 + 2\sigma_\theta^2 - R^2(\sigma_\theta^2 + 2\sigma_z\sigma_\theta))/(2R^2 - 1)]^{0.5}. \quad (15)$$

2.4. Instantaneous strain hardening exponents and instantaneous strength coefficient

The strain hardening exponent 'n' and the strength coefficient 'K' can be determined according to the Ludwik equation [9],

$$\sigma = K\varepsilon^n, \quad (16)$$

where 'σ' is the true stress and 'ε' is the true strain.

It is assumed that the consecutive compressive loads were specified as 1, 2, 3, …, $(m-1)$, m. Now the Eq. (16) can be rewritten as:

$$\sigma_m = K(\varepsilon_m)^n, \quad (17)$$

$$\sigma_{m-1} = K(\varepsilon_{m-1})^n. \quad (18)$$

Subtracting Eq. (17) from Eq. (16),

$$(\sigma_m - \sigma_{m-1}) = K[(\varepsilon_m)^n - (\varepsilon_{m-1})^n]. \quad (19)$$

Eq. (19) can be further simplified as,

$$K = \left[\frac{(\sigma_m - \sigma_{m-1})}{[(\varepsilon_m)^n - (\varepsilon_{-1})^n]}\right]. \quad (20)$$

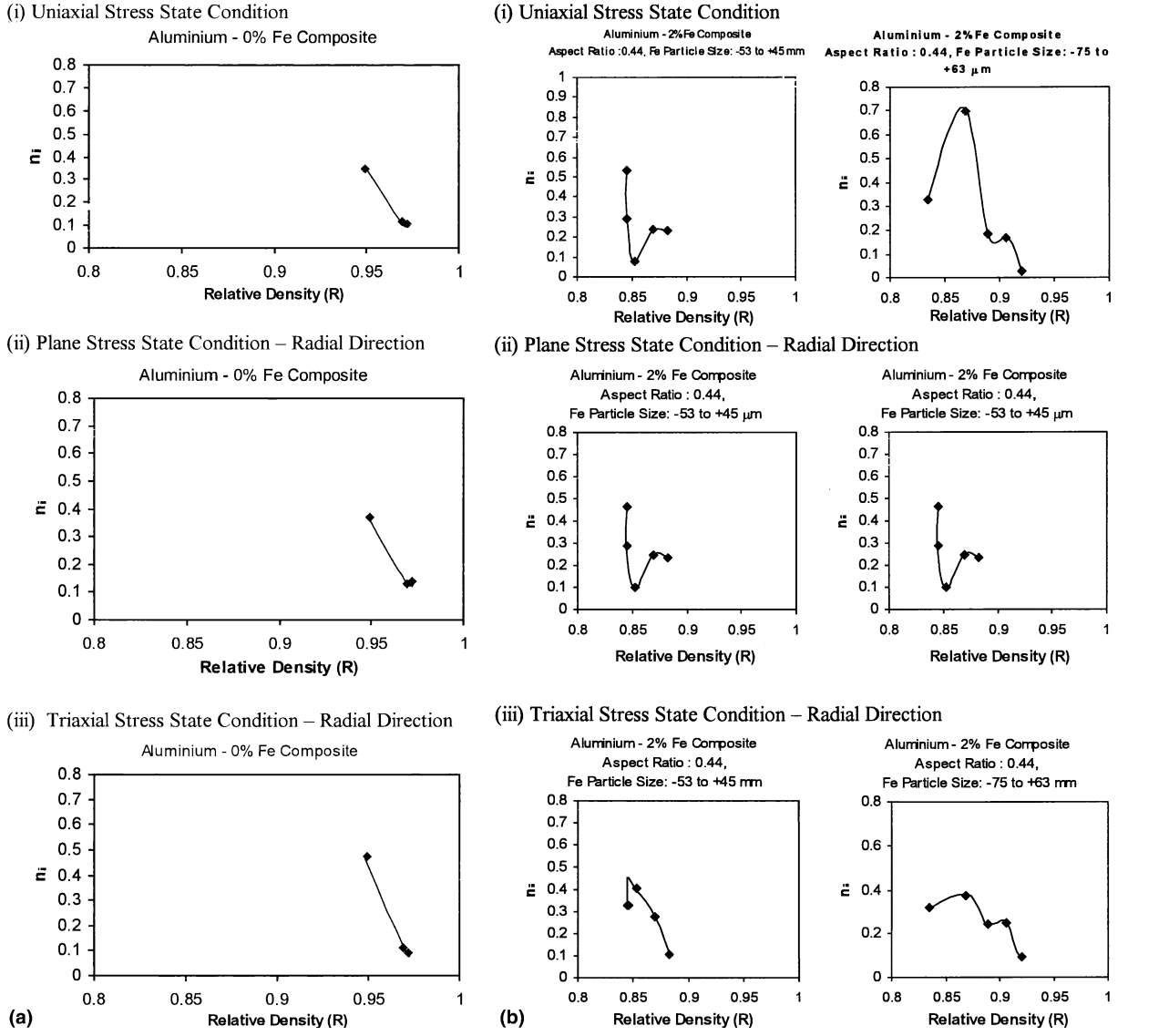

Fig. 5. Strain hardening exponent (n_i) vs. relative density (R) for various stress state conditions: (a) Al–0% Fe composite; (b) Al–2% Fe composite with aspect ratio 0.44; (c) Al–2% Fe composite with aspect ratio 0.45; (d) Al–2% Fe composite with aspect ratio 0.75.

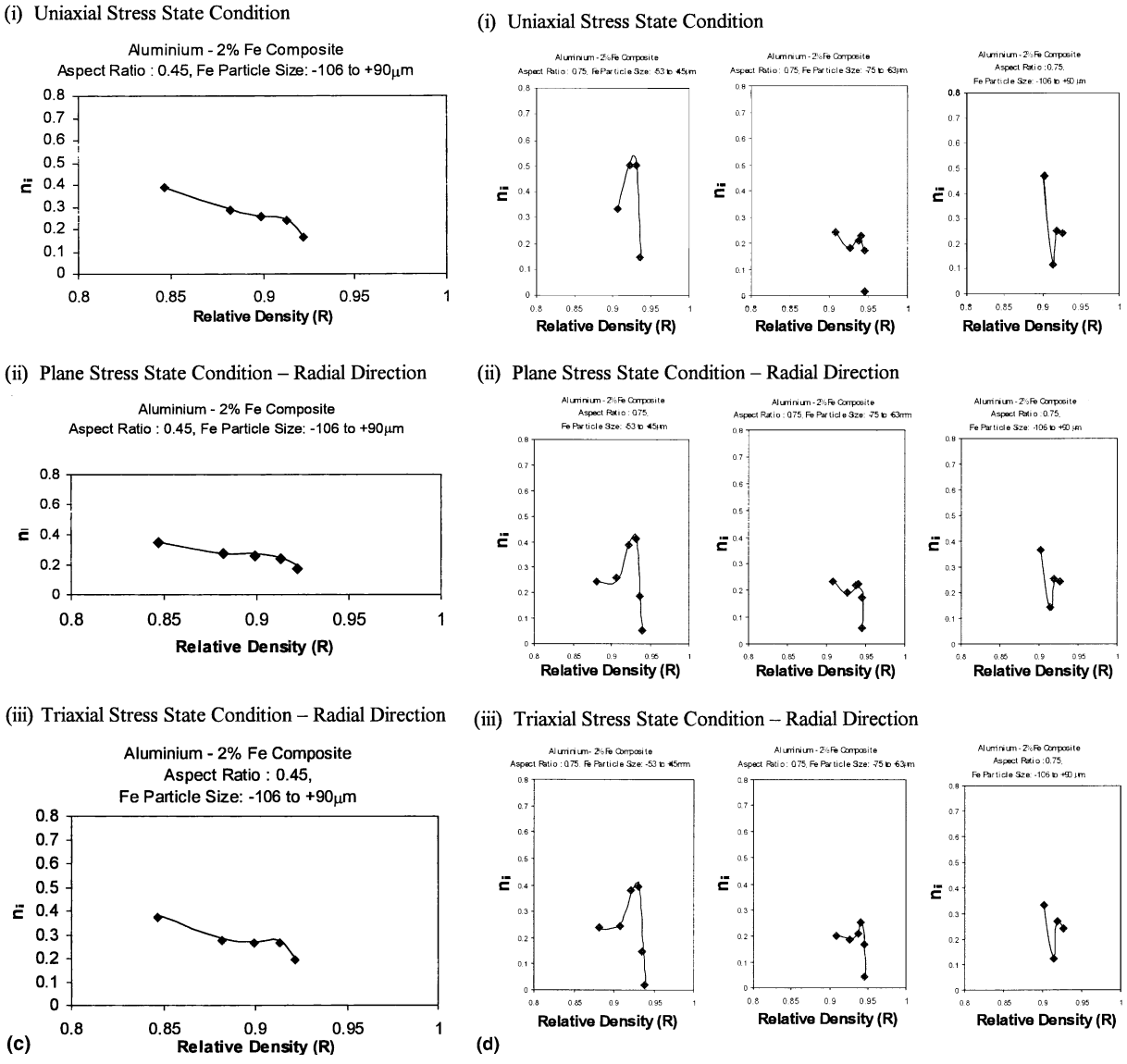

Fig. 5 (*continued*)

Now dividing the Eq. (17) by Eq. (18), the following expressions can be obtained,

$$(\sigma_m/\sigma_{m-1}) = (\varepsilon_m)^n/(\varepsilon_{m-1})^n. \quad (21)$$

Taking natural logarithm on both sides of the above equation, it leads to find the value of '*n*',

$$n = \ln[(\sigma_m/\sigma_{m-1})]/\ln[(\varepsilon_m)/(\varepsilon_{m-1})]. \quad (22)$$

From the Eqs. (20) and (22) the instantaneous strain hardening exponent '*n*' and the instantaneous strength coefficient '*K*' can be calculated.

3. Experimental details

Atomized aluminium and iron powders of the characterization stated in the Table 1 was procured and analyzed for its purity level. The purity level of the aluminium and iron powders was found to be 99.7% and 99.62%, respectively. The compacts were prepared from the aluminium and iron powders with different aspect ratios at the compacting pressure range of 200–225 MPa in order to obtain the initial perform density ranging from 0.85 to 0.92 of the theoretical value. The powder metal compacts were prepared by blending aluminium and iron powders of different iron contents namely 0% and 2% with iron particle sizes of −53 to +45 μm, −76 to +63 μm and −106 to +90 μm for three different aspect ratios namely 0.44, 0.45 and 0.75. The ceramic coating was applied over the surface of the compacts to protect them from oxidation during sintering. The ceramic-coated compacts were sintered in an electric muffle furnace at 500 °C for a period of 60 min. After the completion of the

sintering schedule, the compacts were allowed to cool at room temperature by switching off the furnace power supply.

The sintered performs were cleaned from the sand particles and the dimensional measurements made before and after each deformation. The deformation of the compact was carried out between two flat open dies hardened to Rc 50–55 and tempered to Rc 46–50 on 100 tons capacity hydraulic press. Each compacts was applied with the compressive loading in the step of 0.01 MN until the appearance of first visible cracks on the free surface. Immediately after the completion of each step of loading, the deformed height, the contact diameters, the bulged diameter and the density were measured.

4. Results and discussion

Fig. 1 has been plotted between the axial stress (σ_z) and the true axial strain (ε_z) for different aspect ratios, different iron content (ranges from 0% to 2%) and different iron particle sizes. It is observed that the flow stress and the axial strain values increased to higher value when alloying addition of iron is made. When the aspect ratio is small (0.44), the sintered compact with smaller iron particle size (−53 to +45 μm) shows the higher axial strain obtained before fracture and compact with medium iron particle size (−75 to +63 μm) experiences the higher flow stress during cold upsetting. For the aspect ratio of 0.75, the axial flow stress is high when the iron particle size is fine (−53 to +45 μm) and the axial strain

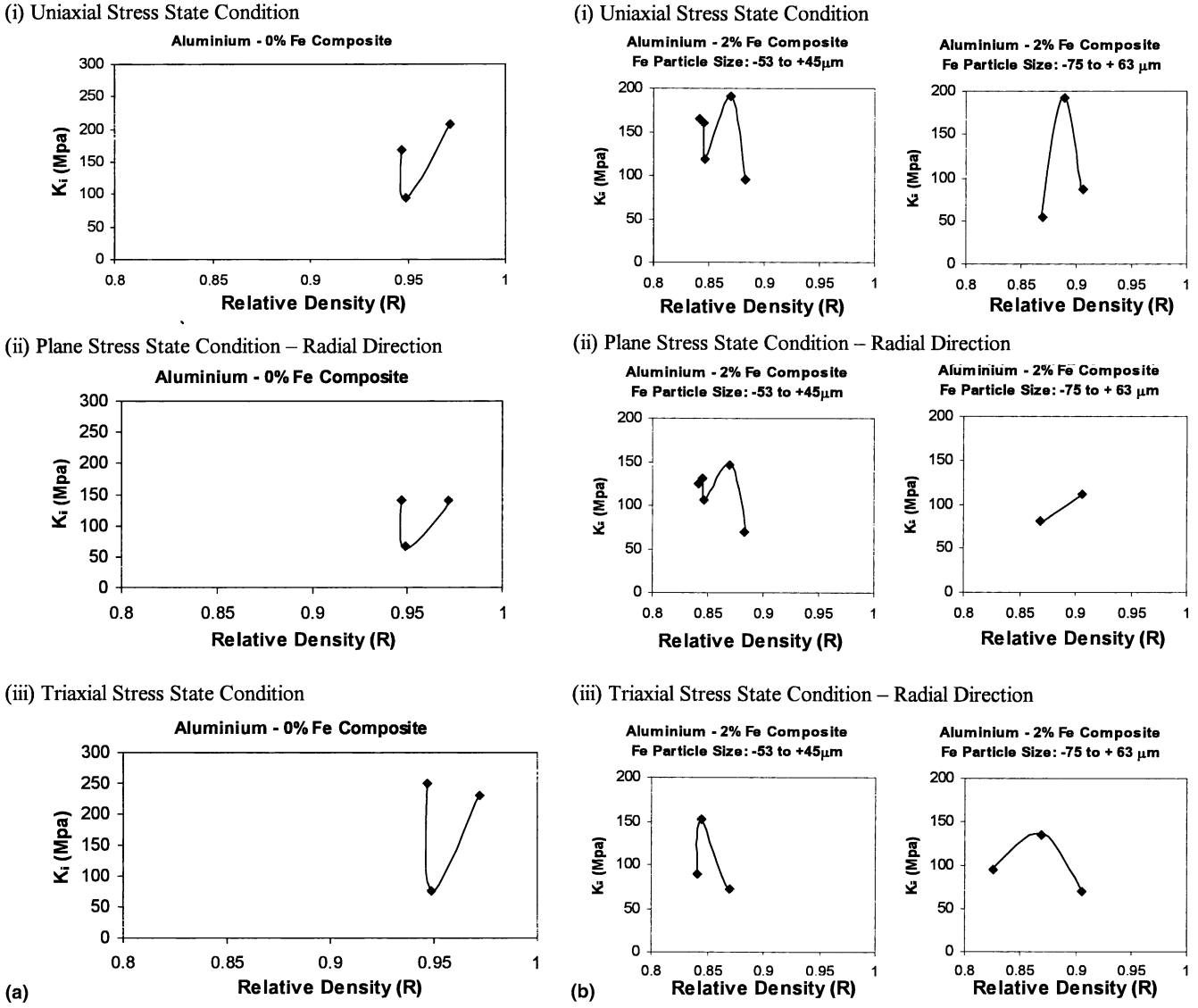

Fig. 6. Strength coefficient (K) vs. relative density (R) for various stress state condition: (a) Al–0% Fe composite; (b) Al–2% Fe composite with aspect ratio 0.44; (c) Al–2% Fe composite with aspect ratio 0.45; (d) Al–2% Fe composite with aspect ratio 0.75.

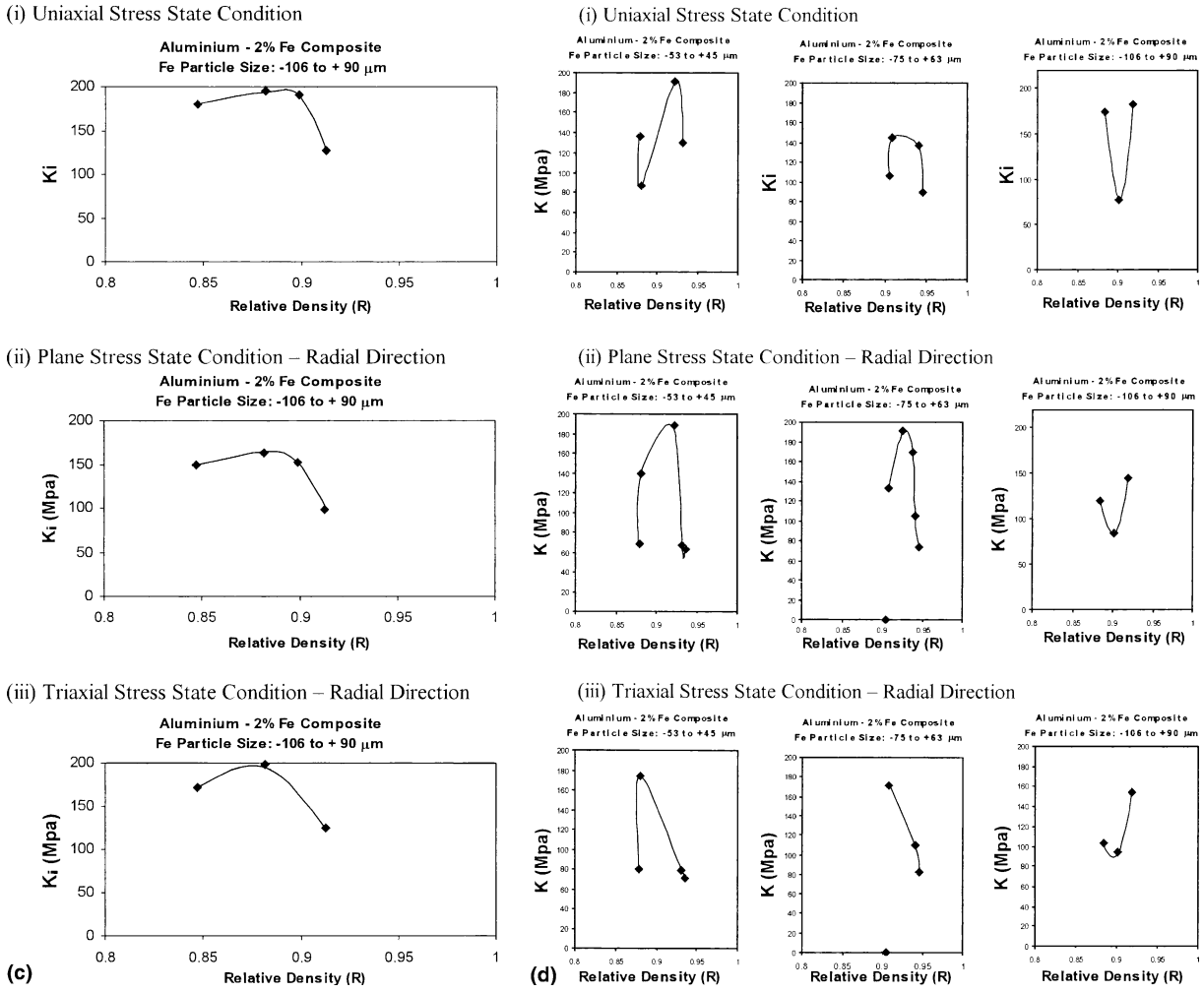

Fig. 6 (*continued*)

reduces to a low value when the iron particle size is coarse (−106 to +90 μm).

Fig. 2 has been drawn between the hoop stress (σ_θ) [according to (a) plane stress and (b) triaxial state of stress] and the hoop strain (ε_θ) for the different aspect ratios, iron content and the iron particle sizes. It is generally noted that the hoop stress determined according to the triaxial state of stress is always higher than that obtained for the case of plane stress condition. As the hoop strain increases, the difference between hoop stresses (according to triaxial stress state and plane stress state) increases. When alloying addition of iron is made together with aluminium, the hoop stress and the hoop strain increases to higher value. When the coarser size of iron particle (−106 to +90 μm) is added, the hoop stress and the hoop strain values decrease.

The behaviour shown in Fig. 3 is same as the behaviour observed in the Fig. 2. Fig. 4 has been plotted between the hydrostatic stress (σ_m) and the axial strain (ε_z) for different aspect ratios, different iron content and different iron particle sizes. For triaxial state of stress, the hydrostatic stress is found to be tensile in nature and the same is found to be compressive in nature for plane stress state. The hydrostatic stress for the triaxial state of stress increases with increasing amount of the axial strain, where as in the case of plane stress state condition, the hydrostatic stress remains almost constant.

Fig. 5(a)–(d) have been drawn between the instantaneous strain hardening exponent (n_i) and the relative density (R) for various stress state conditions namely uniaxial, plane stress and triaxial stress state. It is observed that the stress state alters the value of the instantaneous strain hardening exponent (n_i). When iron is added, the instantaneous strain hardening exponent value (n_i) decreases with increase in the relative density. The shape of the plot completely changes when the stress state is altered. When the particle size is large (−106 to +90 μm), the strain hardening exponent value (n_i) decreases very slowly with increase in the relative density and this behaviour is different when compared with the other smaller particle sizes. When the aspect

ratio changes to higher value (0.75), the nature of the plot between the strain hardening exponent value (n_i) and the relative density (R) is completely changed.

Fig. 6(a)–(d) have been drawn between the instantaneous strength coefficient value (K_i) and the relative density (R) for different aspect ratios, different iron content and different iron particle sizes. As observed in the case of Fig. 5, the Fig. 6 shows that the plot between the instantaneous strength coefficient (K_i) and the relative density (R) is completely changed for the triaxial state of stress. For the case of uniaxial stress state condition, the value of the K_i is found to be very high compared with other two stress state conditions in the case of lower iron particle sizes. When the iron particle size is large (−106 to +90 μm), the instantaneous strength coefficient value K_i in uniaxial and triaxial stress state condition is almost same. When the aspect ratio is increased to 0.75, the nature of plot between the instantaneous strength coefficient value (K_i) and the relative density (R) is completely changed.

5. Conclusion

- The flow stress and the axial strain value increases to higher value when alloying addition of iron is made.
- For the smaller aspect ratio and iron particle size of the sintered compacts, the higher axial strain is obtained before fracture.
- The hoop stress obtained in the triaxial stress state is always higher than that obtained for the other two stress state conditions. As the axial strain increases, the difference between the hoop stresses (according to triaxial and plane stress state conditions) increases.
- The hydrostatic stress in the triaxial state of stress is found to be tensile in nature and the same is found to be compressive in the plane stress state conditions.
- The stress state alters the nature of relationship between the instantaneous strain hardening exponent value and the relative density.
- The instantaneous strength coefficient value (K_i) for a smaller iron particle size is very high in the case of uniaxial stress condition compared with other two stress state conditions, for lower aspect ratio. For higher aspect ratio, the behaviour between the above is completely changed.

References

[1] Dieter George E. Mechanical metallurgy. McGraw Hill book Company; 1988.
[2] Kuhn HA, Downey CL. Deformation characteristics and plasticity theory of sintered powder materials. Int J Powder Metall 1971;7(1):15–25.
[3] Green RJ. A plasticity theory for porous solids. Int J Mech Sci 1972;14:215–24.
[4] Shima S, Oyane M. Plasticity theory for porous metals. Int J Mech Sci 1976;18:285–91.
[5] Gurson AL. Continuum theory of ductile rupture by void nucleation and growth: Part I – yield criteria and flow rules for porous ductile media. J Eng Mater Technol Trans ASME 1977:1–9.
[6] Doraivelu SM, Gegel HL, Gunasekara JS, Malas JC, Morgan JT. A new yield function for compressible P/M materials. Int J Mech Sci 1984;26(9/10):527–35.
[7] Abdel-Rahman M, EI-Sheikh MN. Workability in forging of powder metallurgy compacts. J Mater Process Technol 1995;54:97–102.
[8] Abdel-Rahman M. Determination of workability curves using two mechanical tests. J Mater Process Technol 1995;51: 50–63.
[9] Narayanasamy R, Pandey KS. Some aspects of work hardening in sintered aluminium–iron composite preforms during cold axial forming. J Mater Process Technol 1998;84:136–42.
[10] Inigoraj AJR, Narayansamy R, Pandey KS. Strain-hardening behaviour of sintered aluminium–3.5% alumina composite preforms during axial compression with and without annealing. J Mater Process Technol 1998;84:143–8.
[11] Selvakumar N, Narayanasamy R. Phenomenon of strain hardening behaviour of sintered aluminium preforms during cold axial forming. J Mater Process Technol 2003;142:347–54.
[12] Senthilvelan T, Raghukandan K, Venkatraman A. Modeling of process parameters on the working of P/M copper preforms. J Mater Process Technol 2003;142:767–72.
[13] Peng X, Balendra R. Application of physically based constitutive model to metal forming analysis. J Mater Process Technol 2004;145:180–8.
[14] Vujovic V, Shabaik AH. A new workability criterion for ductile metals. J Eng Mater Technol 1986;108:245–9.
[15] Narayansamy R, Pandey KS. A study of barreling aspects on P/M iron preforms during hot upset forming. J Mater Process Technol 2000;100:87–94.
[16] Narayanasamy R, Ponalagusamy R. Unpublished report on P/M forging, National Institute of Technology, Tiruchirappalli 620 015, Tamilnadu, India; 2001.